

Differentiating the Higgs Boson from the Dilaton and Radion at Hadron Colliders

Vernon Barger, Muneyuki Ishida,* and Wai-Yee Keung†

Department of Physics, University of Wisconsin, Madison, Wisconsin 53706, USA

(Received 21 November 2011; published 8 March 2012)

A number of candidate theories beyond the standard model (SM) predict new scalar bosons below the TeV region. Among these, the radion, which is predicted in the Randall-Sundrum model, and the dilaton, which is predicted by the walking technicolor theory, have very similar couplings to those of the SM Higgs boson, and it is very difficult to differentiate these three spin-0 particles in the expected signals of the Higgs boson at the LHC and Tevatron. We demonstrate that the observation of the ratio $\sigma(\gamma\gamma)/\sigma(WW)$ gives a simple and decisive way to differentiate these, independent of the values of model parameters, the vacuum expectation values of the radion, and dilaton fields.

DOI: 10.1103/PhysRevLett.108.101802

PACS numbers: 14.80.Bn, 13.85.Qk, 14.80.Ec

A number of candidate theories beyond the standard model (SM) predict new scalar bosons below the TeV region. When a scalar boson signal is detected in the Higgs search at the LHC, it is very important to determine whether it is really a SM Higgs boson or another exotic scalar. Among these, the radion (R), predicted in the Randall-Sundrum (RS) model [1–18], and the dilaton (D), predicted in spontaneous scale symmetry breaking [19–25], have very similar couplings to those of the standard model Higgs boson (H), and it is very difficult to differentiate these three particles, DHR , in the signals. A distinctive difference [17,19,26,27] is in their couplings to massless gauge bosons. We demonstrate that the ratios $\sigma(\gamma\gamma)/\sigma(WW)$ are different from each other, and their observation gives a decisive method to distinguish these three spin-0 particles. Our main result is given in Fig. 2. It is important that the $\sigma(\gamma\gamma)/\sigma(WW)$ ratio must be independent of the model parameters; the VEVs of the radion and dilaton fields. The test applies to both LHC and Tevatron experimental searches.

For definiteness we consider the dilaton coupling given in Ref. [19], which is the same as the dilaton coupling in four-dimensional walking technicolor theory [21–25] where all SM fields are composites of strongly interacting fields in conformal field theory (CFT). In AdS/CFT correspondence this dilaton is dual to the radion [2–4] in the original Randall-Sundrum (RS1) model [1], where all the SM fields are localized at the infrared (IR) brane in the five-dimensional anti-de Sitter (AdS) space background. We consider the radion coupling of the Randall-Sundrum (RS2) model given in Ref. [5] where all the SM fields are in the bulk [6–18]. The radion has bulk couplings to the gauge bosons. It is dual [5] to the dilaton in CFT. We do not consider flavor changing neutral current (FCNC) processes; however, we note that a dilaton in a particular CFT with SM fields that are elementary and weakly coupled can generically have FCNC [28,29], as can the radion of the RS2 model [30] considered here. We will

study collider signatures from the gauge coupling differences of DHR in the following.

Effective Lagrangians.—We treat the SM Higgs boson H , the radion R , and the dilaton D , which are also denoted as $(\varphi^i) = (\varphi^1, \varphi^2, \varphi^3) = (h^0, \phi, \chi) \equiv (H, R, D)$. The vacuum expectation values (VEV) of these fields are denoted as

$$(F_i) = (F_1, F_2, F_3) = (-v, \Lambda_\phi, f) \quad (1)$$

for H , R , and D , respectively. The F_i^{-1} determine overall coupling strengths of these particles, and $F_1 = -v = -246$ GeV.

The Lagrangian L_{eff} of the interactions [3–5,14,16,19] with the SM particles is given by

$$L_{\text{eff}} = L_A + L_V + L_f + L_h + L_{AV}, \quad (2)$$

$$L_A = -\frac{\varphi^i}{4F_i} \left[\left(\frac{1}{kL} + \frac{\alpha_s}{2\pi} b_{\text{QCD}}^i \right) \sum_a F_{\mu\nu}^a F^{a\mu\nu} + \left(\frac{1}{kL} + \frac{\alpha}{2\pi} b_{\text{EM}}^i \right) F_{\mu\nu} F^{\mu\nu} \right], \quad (3)$$

$$L_V = -\frac{2\varphi^i}{F_i} \left[\left(m_W^2 W_\mu^+ W^{-\mu} + \frac{1}{4kL} W_{\mu\nu}^+ W^{-\mu\nu} \right) + \left(\frac{m_Z^2}{2} Z_\mu Z^\mu + \frac{1}{8kL} Z_{\mu\nu} Z^{\mu\nu} \right) \right], \quad (4)$$

$$L_{AV} = -\frac{\varphi^i}{F_i} \frac{\alpha}{4\pi} b_{Z\gamma}^i F_{\mu\nu} Z^{\mu\nu}, \quad (5)$$

$$L_f = \frac{\varphi^i}{F_i} \sum_f I_f^i m_f \bar{f} f, \quad (6)$$

$$L_h = \frac{\varphi^i}{F_i} (2m_h^2 h^2 - \partial_\mu h \partial^\mu h), \quad (7)$$

where L denotes the separation of the branes in the RS2 model and kL is a parameter that governs the weak scale-Planck scale hierarchy. The $1/kL$ term is absent for the

TABLE I. gg and $\gamma\gamma$ couplings, $\frac{1}{kL} + \frac{\alpha_s}{2\pi} b_{\text{QCD}}^i$ (second row) and $\frac{1}{kL} + \frac{\alpha}{2\pi} b_{\text{EM}}^i$ (third row), of DHR scalars: only the third column contributes for H where $F_t(F_W)$ represent the triangle-loop contributions of top quark and W boson which are given in Refs. [31–33]. For D , both second and third columns contribute where the second column represents the trace anomaly. For R the first column ($1/kL$) also contributes. It comes from the bulk-field coupling, The volume of the fifth dimension is taken to be $kL = 35$ in R , while we can represent D, H with $(1/kL) \rightarrow 0$.

R	D, R	D, R, H
$\frac{1}{kL}$	$+\frac{\alpha_s}{2\pi}(11 - \frac{2}{3}6)$	$+\frac{\alpha_s}{2\pi}F_t; F_t = \begin{cases} \frac{2}{3} & m < 2m_t \\ 0 & 2m_t < m \end{cases}$
$\frac{1}{kL}$	$+\frac{\alpha}{2\pi}(\frac{19}{6} - \frac{41}{6})$	$+\frac{\alpha}{2\pi}(\frac{8}{3}F_t - F_W); \frac{8}{3}F_t - F_W = \begin{cases} -\frac{47}{9} & m < 2m_W \\ -\frac{2}{9} & 2m_W < m < 2m_t \\ -2 & 2m_t < m \end{cases}$

dilaton and the Higgs boson. L_A specifies the couplings to the massless gauge bosons, and $F_{\mu\nu}^a(F_{\mu\nu})$ represents the field strength of gluon (photon). L_V gives the couplings to the weak bosons, and $W_{\mu\nu}^+ = \partial_\mu W_\nu^+ - \partial_\nu W_\mu^+$, etc. In the fermion-coupling Lagrangian L_f , the factors are $I_f^H = -1$ and $I_f^D = 1$ for all fermions f , while the I_f^R depend upon the bulk wave functions of the fermion f in the RS2 model. We take $I_b^R = 1.66$ for one value of $b\bar{b}$ coupling [15] as our example. L_h represents the couplings to the Higgs boson. L_h is also applicable to the $\varphi^i = R, D$. In the radion effective interaction, the brane kinetic terms are taken to be zero [16].

A distinction in Eq. (3) is the gg and $\gamma\gamma$ couplings $\frac{1}{kL} + \frac{\alpha_{s,EM}}{2\pi} b_{\text{QCD,EM}}^i$. Their expressions are given in Table I. $b_{\text{QCD,EM}}^i$ is given by the sum of the triangle-loop contributions of top quark and W boson and the β function coefficient appearing in the trace anomaly of the SM energy-momentum tensor $T_{\mu\nu}(SM)$ [2,4,19,25]. The trace-anomaly term contributes for R and D but not for H . Here we should note that the β function contributions (the second column) always count all favors “light or heavy.” But, the mass-coupling term of the triangle-loop diagram operates in a way to cancel the heavy countings if

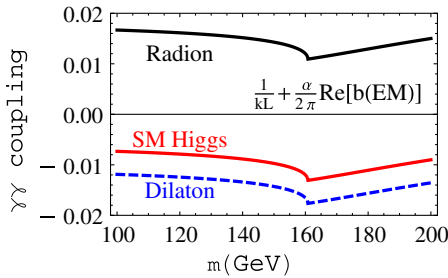


FIG. 1 (color online). The real part of the $\gamma\gamma$ couplings, $\frac{1}{kL} + \frac{\alpha}{2\pi} b_{\text{EM}}^i$ for $i = H, D$, and R . The bulk coupling term is given by $kL = 35$ for R , while $(1/kL) \rightarrow 0$ for D and H . The D has an additional contribution $-\frac{11}{3}$ in b_{EM}^D compared to b_{EM}^H . The R has a contribution from the bulk-field coupling which destructively interferes with the term of $b_{\text{EM}}^R = b_{\text{EM}}^D$. The imaginary parts contribute above the $m > 2m_W$ and they only give subleading contributions.

the D (or R) masses are lower than the corresponding threshold. As a result, $b_{\text{QCD}}^{R,D} = 11 - \frac{2}{3}5$ for $m < 2m_t$ with the number of effective flavors $n_f = 5$. A similar argument is also applicable to $b_{\text{EM}}^{R,D}$.

The real part of the $\gamma\gamma$ couplings is given in Fig. 1. The destructive interference between the bulk coupling term $1/kL$ and the b_{EM}^R term is due to the opposite sign, and this yields the very different shape of $\sigma(\gamma\gamma)/\sigma(WW)$ versus m : the cusp at $m = 2m_W$, which comes from the WW threshold effect, constructively contributes for D and H , and destructively for R . This behavior is seen in Fig. 2.

L_{AV} describes the $Z\gamma$ decays. The effective couplings $b_{Z\gamma}^i$ are given by

$$b_{Z\gamma}^i = -A_W - A_F + \frac{b_{Z\gamma}}{\sin\theta_W \cos\theta_W}, \quad (8)$$

$$b_{Z\gamma} = \frac{19}{6} + \frac{11}{3} \sin^2\theta_W,$$

where R, H, D have both A_W and A_F terms from the triangle-loop contributions of W and SM fermions, respectively. Their explicit forms are given in Refs. [31,32]. A_F is negligible compared to A_W . The third term comes from the trace anomaly of $T_{\mu\nu}^\mu(SM)$ and it contributes to R, D , but not to H . We can check that particles with heavier thresholds than m_D or m_R decouple also in $Z\gamma$. To a good approximation the bulk-field coupling of R gives no contribution to $Z\gamma$ [34].

$\sigma(\gamma\gamma)/\sigma(WW)$ ratio.—From L_{eff} in Eq. (2), we can calculate the partial widths Γ of H, R , and D . They are proportional to the inverse squares of the overall constants F_i , but the values of F_R and F_D are presently unknown. However, the $\sigma(\gamma\gamma)/\sigma(WW)$ ratios [33] are independent of these VEVs. Figure 2 shows the ratios $\Gamma(\gamma\gamma)/\Gamma(WW) = \sigma(\gamma\gamma)/\sigma(WW)$ (upper figure), the ratios $\Gamma(b\bar{b})/\Gamma(WW) = \sigma(b\bar{b})/\sigma(WW)$ (middle figure), and the ratios $\Gamma(Z\gamma)/\Gamma(WW) = \sigma(Z\gamma)/\sigma(WW)$ (lower figure), for R and D of the same mass. They are compared with those of H of the same mass.

As can be clearly seen in Fig. 2, we can differentiate the three scalars, R, D, H , by observing the ratio $\sigma(\gamma\gamma)/\sigma(WW)$. In Fig. 2 the slope changes around

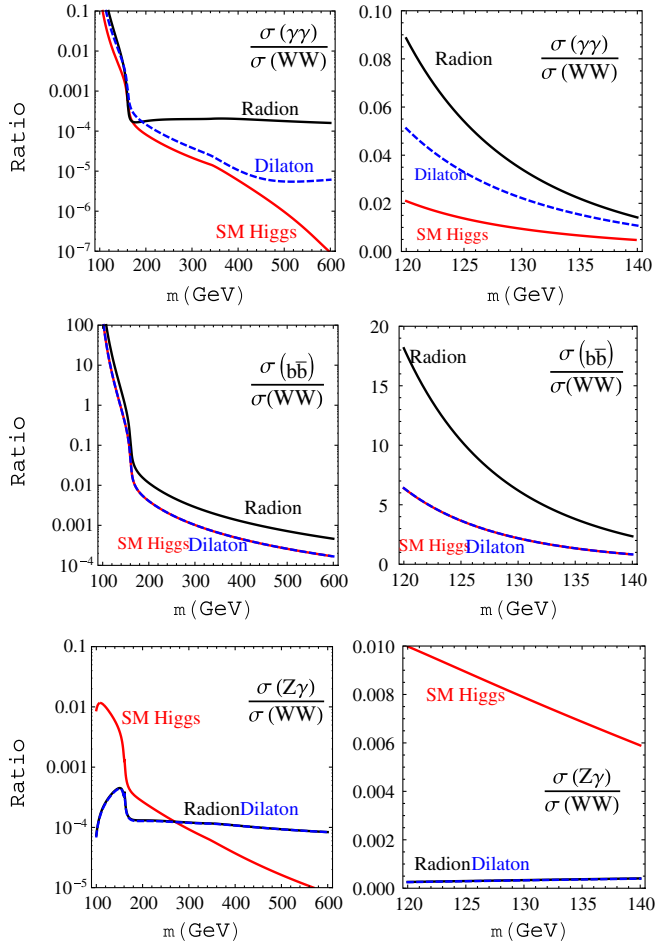


FIG. 2 (color online). The cross section ratios, $\sigma(\gamma\gamma)/\sigma(WW)$ and $\sigma(b\bar{b})/\sigma(WW)$ versus the mass of the scalar: H , R , D . For the radion (black solid), the dilaton (blue dashed), and the SM Higgs boson (red dotted) for $\sigma(\gamma\gamma, b\bar{b}, Z\gamma)/\sigma(WW)$ (upper, middle, lower figures). The ratios are independent of the values of the model parameters, F_R and F_D . H and D have the same value of $\sigma(b\bar{b})/\sigma(WW)$ while for R it can be different, since the ratio is proportional to the square of the parameter I_b^R that is taken to be 1.66 as an example. $\sigma(Z\gamma)/\sigma(WW)$ of R and D are different from that of H due to the trace-anomaly contribution.

$m \simeq 2m_W$ since $\Gamma(WW)$ steeply decreases below the WW threshold. The R gives an almost constant ratio in $m_R > 2m_W$ because of the contribution from the bulk coupling term $1/kL$ which is energy independent. The drastic change in slope of the ratio of R near $m \simeq 2m_W$ occurs from the interference between this bulk coupling and the trace-anomaly term. See, Fig. 1.

The ratio $\sigma(b\bar{b})/\sigma(WW)$ of R can differ from H and D , because of the parameter I_b^R , so measuring this quantity is also helpful to distinguish R from the other two scalars.

The ratio $\sigma(Z\gamma)/\sigma(WW)$ of R and D can differ from H , because of the trace-anomaly contributions. This channel is helpful to determine the coupling form of the signal. It may be possible to detect it by focusing on the monochromatic photon spectrum from $H \rightarrow Z\gamma$.

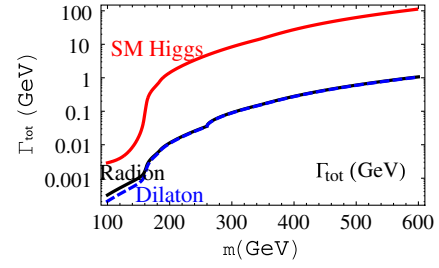


FIG. 3 (color online). The total widths (GeV) of the radion R (black solid), dilaton D (blue dashed), and SM Higgs boson H (red dotted). $\Gamma_{\text{tot}}^R, \Gamma_{\text{tot}}^D$ scale with $(v/F_R)^2, (v/F_D)^2$, respectively, where F_R and F_D are commonly taken to be 3 TeV.

Total widths and decay branching fractions (BF).—The total widths of R, D, H are given in Fig. 3. $\Gamma_{\text{tot}}^R, \Gamma_{\text{tot}}^D$ scale with $(v/F_R)^2[(v/F_D)^2]$ where $F_R = F_D = 3$ TeV are taken, and the R and D widths are about 2 orders of magnitudes smaller than the Γ_{tot}^H with the same mass.

The branching fractions (BF) of the decays to $\bar{X}X = WW, \gamma\gamma, b\bar{b}, gg, Z\gamma$ are compared in Fig. 4, where the K factor in NNLO [35] is considered for gg . $\text{BF}(\gamma\gamma)$ shows very delicate structures. $\text{BF}(H \rightarrow \gamma\gamma)$ is the largest at $m < 2m_W$, since the H has the smallest couplings to gg and the main H decay mode in this energy region is $b\bar{b}$.

Concluding remarks.—The measurement of the ratio [36] $\sigma(\gamma\gamma)/\sigma(WW)$ provides a decisive way to differentiate the radion R , the dilaton D , and the SM Higgs boson H . It is only necessary to count the event numbers of $\gamma\gamma$ and WW decays of an observed signal. This method is independent of the values of the model parameters, the VEVs F_R and F_D . It applies to both the LHC and Tevatron experimental searches.

The scalars are also expected to be produced in W/Z associated production, $W^* \rightarrow W\varphi^i$ and $Z^* \rightarrow Z\varphi^i$. The production cross section $\sigma_{\text{assoc}}(D)$ and $\sigma_{\text{assoc}}(R)$ are smaller than $\sigma_{\text{assoc}}(H)$, respectively, by the factors $(\frac{1}{F_D})^2$ and $(\frac{1}{F_R})^2$, which are ~ 0.01 in the $F_D \sim F_R \sim 3$ TeV case. This small cross section of associated production also can be used to differentiate the R and D from H [27].

The production of D and R via the WW, ZZ fusion subprocess is much smaller than that of H , due to their relatively smaller decay widths to WW and ZZ .

We may also consider the scenario that both D and H (or R and H) exist with comparable masses in the region $m \sim 125$ GeV, where the ongoing Higgs search data show some excess over the expected SM cross section. At this mass both $D(R)$ and H have very narrow widths, and their resonance peaks will be smeared by experimental resolution into one with twice the production cross section, even with the mixing of scalars taken into account. In this case the $\sigma(\gamma\gamma)/\sigma(WW)$ ratio will be intermediate between the single-state values. Another possible scenario is that R or D mix [4,37–39] with H . Then, the lighter scalar can have a

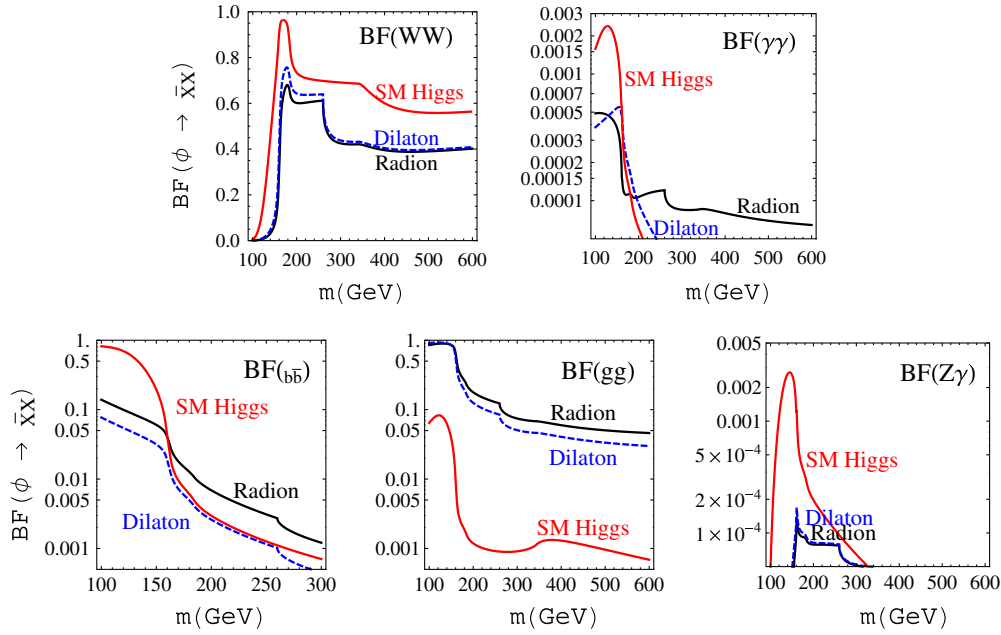


FIG. 4 (color online). Branching fractions (BF) of the decays to $\bar{X}X = WW, \gamma\gamma, \bar{b}b, gg, Z\gamma$: for the radion R (black solid), the dilaton D (blue dashed), and the SM Higgs H (red dotted) in each figure. This result is independent of the model parameters, F_R for the radion and the F_D for the dilaton. For $\text{BF}(\bar{b}b)$, I_b^R is taken to be 1.66 as an example.

mass below 100 GeV and its production will be suppressed compared to that of the SM Higgs boson.

For dilaton or radion masses much larger than $2m_W$, the narrow width makes discovery in WW and ZZ easier than for the SM Higgs boson [27].

Finally, our study applies also to generic singlet models [40]. The singlet decouples from SM particles and the phenomenology is dependent on the amount of mixing of H with the singlet scalar. The H production cross section can be significantly smaller by the mixing effect, and thus, a low-mass Higgs boson with $m_H < 100$ GeV also become possible.

We thank Professor Bill Bardeen and Professor Misha Stephanov for discussions. M.I. is very grateful to the members of phenomenology institute of University of Wisconsin-Madison for their hospitality. This work was supported in part by the U.S. Department of Energy under Grants No. DE-FG02-95ER40896 and No. DE-FG02-84ER40173, in part by KAKENHI [2274015, Grant-in-Aid for Young Scientists (B)], and in part by grant as Special Researcher of Meisei University.

*Department of Physics, Meisei University, Hino, Tokyo 191-8506, Japan.

†Department of Physics, University of Illinois, Chicago, IL 60607, USA.

- [1] L. Randall and R. Sundrum, *Phys. Rev. Lett.* **83**, 3370 (1999).
- [2] W. D. Goldberger and M. B. Wise, *Phys. Rev. Lett.* **83**, 4922 (1999); *Phys. Lett. B* **475**, 275 (2000).
- [3] Kingman Cheung, *Phys. Rev. D* **63**, 056007 (2001).

- [4] G. F. Giudice, R. Rattazzi, and J. D. Wells, *Nucl. Phys.* **B595**, 250 (2001).
- [5] C. Csáki, J. Hubisz, and S. J. Lee, *Phys. Rev. D* **76**, 125015 (2007).
- [6] H. Davoudiasl, J. L. Hewett, and T. G. Rizzo, *Phys. Lett. B* **473**, 43 (2000).
- [7] A. Pomarol, *Phys. Lett. B* **486**, 153 (2000).
- [8] Y. Grossman and M. Neubert, *Phys. Lett. B* **474**, 361 (2000).
- [9] T. Gherghetta and A. Pomarol, *Nucl. Phys.* **B586**, 141 (2000).
- [10] K. Agashe, A. Delgado, M. J. May, and R. Sundrum, *J. High Energy Phys.* **08** (2003) 050.
- [11] K. Agashe, R. Contino, and A. Pomarol, *Nucl. Phys.* **B719**, 165 (2005).
- [12] C. Csaki, C. Grojean, L. Pilo, and J. Terning, *Phys. Rev. Lett.* **92**, 101802 (2004).
- [13] C. Csaki, M. L. Graesser, and G. D. Kribs, *Phys. Rev. D* **63**, 065002 (2001).
- [14] T. Han, G. D. Kribs, and B. McElrath, *Phys. Rev. D* **64**, 076003 (2001).
- [15] H. Davoudiasl, G. Perez, and A. Soni, *Phys. Lett. B* **665**, 67 (2008).
- [16] H. Davoudiasl, T. McElmurry, and A. Soni, *Phys. Rev. D* **82**, 115028 (2010).
- [17] M. Frank, B. Korutlu, M. Toharia, *Phys. Rev. D* **84**, 115020 (2011).
- [18] V. Barger and M. Ishida, arXiv:1110.6452.
- [19] W. D. Goldberger, B. Grinstein, and W. Skiba, *Phys. Rev. Lett.* **100**, 111802 (2008).
- [20] Y. Fujii, “*Gravitation and Scalar Fields*,” Kodansha Scientific, 1997 (in Japanese).
- [21] K. Yamawaki, M. Bando, and K. -i. Matumoto, *Phys. Rev. Lett.* **56**, 1335 (1986).
- [22] T. W. Appelquist, D. Karabali, and L. C. R. Wijewardhana, *Phys. Rev. Lett.* **57**, 957 (1986).

- [23] M. A. Luty and T. Okui, *J. High Energy Phys.* **09** (2006) 070.
- [24] R. Rattazzi, V. S. Rychkov, E. Tonni, and A. Vichi, *J. High Energy Phys.* **12** (2008) 031.
- [25] D. D. Dietrich, F. Sannino, and K. Tuominen, *Phys. Rev. D* **72**, 055001 (2005).
- [26] V. Barger, M. Ishida, and W.-Y. Keung, *Phys. Rev. D* **85**, 015024 (2012).
- [27] B. Coleppa, T. Gregoire, and H.E. Logan, [arXiv:1111.3276v1](https://arxiv.org/abs/1111.3276v1).
- [28] J. Fan, W. D. Goldberger, A. Ross, and W. Skiba, *Phys. Rev. D* **79**, 035017 (2009).
- [29] L. Vecchi, *Phys. Rev. D* **82**, 076009 (2010).
- [30] A. Azatov, M. Toharia, and L. Zhu, *Phys. Rev. D* **80**, 031701 (2009).
- [31] J. F. Gunion, H. E. Harber, G. Kane, and S. Dawson, *Higgs Hunters Guide* (Perseus Books, Cambridge, MA, 2000).
- [32] A. Djouadi, *Phys. Rep.* **457**, 1 (2008).
- [33] V. D. Barger and R. J. N. Phillips, *Collider Physics* (Westview Press, Boulder, CO, 1991), updated ed.
- [34] C. Csaki, J. Erlich, and J. Terning, *Phys. Rev. D* **66**, 064021 (2002).
- [35] S. Catani, D. de Florian, M. Grazzini, and P. Nason, *J. High Energy Phys.* **07** (2003) 028.
- [36] I. Low and J. Lykken, *J. High Energy Phys.* **10** (2010) 053; [arXiv:1005.0872](https://arxiv.org/abs/1005.0872).
- [37] D. Dominici, B. Grzadkowski, J. F. Gunion, and M. Toharia, *Nucl. Phys.* **B671**, 243 (2003).
- [38] M. Toharia, *Phys. Rev. D* **79**, 015009 (2009).
- [39] H. de Sandes and R. Rosenfeld, [arXiv:1111.2006v1](https://arxiv.org/abs/1111.2006v1) [*Phys. Rev. D* (to be published)].
- [40] See, e.g., V. Barger, P. Langacker, and G. Shaughnessy, [arXiv:10611239](https://arxiv.org/abs/10611239); *Phys. Rev. D* **75**, 055013 (2007).